

# Influence of Anodization Parameters in the TiO<sub>2</sub> Nanotubes Formation on Ti-7.5Mo Alloy Surface for Biomedical Application

Ana Lúcia Escada<sup>a,\*</sup>, Roberto Zenhei Nakazato<sup>a</sup>, Ana Paula Rosifini Alves Claro<sup>a</sup>

<sup>a</sup>Departamento de Materiais e Tecnologia, Faculdade de Engenharia Guaratinguetá, Universidade Estadual Paulista “Júlio de Mesquita Filho”, Av. Dr. Ariberto Pereira da Cunha, 333, Parque Alberto Bayington, Guaratinguetá, SP, Brazil

Received: July 11, 2016; Revised: June 28, 2017; Accepted: July 03, 2017

In this study, the effects of the parameters such as applied potential difference, time and annealing temperature in the titania nanotubes formation were evaluated. The morphology of the nanotubes was evaluated by using Field Emission Gun - Scanning Electron Microscope (FEG-SEM), Atomic Force Microscope (AFM), contact angle and X-rays diffraction (XRD). Self-organized nano-structures were formed on the Ti-7.5Mo alloy surface from the same electrolyte (glycerol/NH<sub>4</sub>F) for all conditions. It was observed that the potential influenced the diameter while the length was changed according to the anodization time length. The presence of the phases anatase and rutile was altered by annealing temperature. Results showed that 20V-48h-450 °C was the better than other conditions for application as biomaterial.

**Keywords:** Titanium oxide, Nanotubes, Anodic oxidation, Heat treatment

## 1. Introduction

Titanium (Ti) and its alloys are widely used to manufacture dental implants, maxillofacial, and orthopedic prostheses due to their excellent mechanical properties, low specific weight, high resistance to corrosion, and high biocompatibility<sup>1,2</sup>. Titanium based alloys with different compositions such as Ti-7.5Mo<sup>3,4</sup>, Ti-10Mo<sup>5,6</sup>, Ti-15Mo<sup>7</sup>, Ti-29Nb-13Ta-4.6Zr<sup>8</sup> and Ti-13Nb-13Zr<sup>9</sup> have been studied for biomedical applications. Lin et al.<sup>8,9</sup> developed a binary alloy, Ti-7.5Mo, with a low elastic modulus and a high strength/modulus ratio. A significant difference in elastic modulus between implants and bone tissue can lead to stress, and thereby may cause poor osseointegration, while an implant with a low elastic modulus can facilitate bone growth<sup>10</sup>. Over the past decade, various techniques such as sol-gel method<sup>11</sup>, hydrothermal method<sup>12</sup>, photo oxidation reaction<sup>13</sup>, electro spinning method<sup>14</sup> and anodization<sup>15,16</sup> of titanium surface modification have been employed to fabricate implant surfaces. These techniques are used to promote osseointegration, faster healing time, higher bone-to-implant contact ratio and longevity of titanium implants<sup>17</sup>.

Anodization is an electrolytic passivation technique used to increase the thickness of the natural oxide layer on metal surfaces. This technique has attracted great attention in recent years due to its simplicity as well as the reproducibility of the results obtained<sup>18,19</sup>. The thickness and structure of the oxide layers formed (amorphous or crystalline) depend on the applied potential between the electrodes and duration of anodization process. The structure of the oxide film formed on titanium can be anatase, a mixture of anatase

and rutile, or rutile<sup>20</sup>. Various studies have shown that the heat treatment in TiO<sub>2</sub> nanotubes produces a series of phase changes, eventually developing rutile as the stable phase after heat treatment above ~500 °C<sup>21</sup>.

Bauer et al.,<sup>22</sup> evaluated the influence of anodization potential in the TiO<sub>2</sub> nanotubes growth. The authors observed that the increase of the diameter was directly proportional to the potential increase.

Mohan et al.,<sup>23</sup> investigated the formation of self-organized TiO<sub>2</sub> nanotubes layers by anodic oxidation on Ti-6Al-7Nb alloy for 1 hour at 10, 20 and 30 V in an electrolyte consisting of 1 M H<sub>2</sub>SO<sub>4</sub> and 0.08 M HF. Samples anodized at 10 V exhibited porous structure with diameter of ~35 nm and 250 nm of height. For samples anodized at 20 and 30 V, the nanotubes showed diameters of approximately 100 nm and 125 nm and 30 nm and 35 nm of intertube distance. This indicated that increase in voltage increases the pore diameter. For TiO<sub>2</sub> nanotubes formed by anodizing at 20V, after annealing at 450 °C and 600 °C, the anatase phase was identified. For the samples annealed at 700 °C, rutile phase was observed. The sample annealed at 800 °C contains both anatase and rutile phases, while a rutile phase dominates the sample annealed at 850 °C. The investigations showed that for samples annealed between 450 and 800 °C a tubular morphology was present whereas those annealed at 850 °C showed collapse of nanotubes.

A completely different growth morphology leading to self-organized and ordered nanotubular, nanoporous structures of titania has been obtained when electrolytes containing fluoride ions and suitable anodization conditions are used<sup>20,21</sup>. Recent *in-vitro* study of osteoblasts on anodized

\* e-mail: analuciaescada@uol.com.br

nanotubular titanium substrates has been reported to enhance cell adhesion and proliferation<sup>24</sup>. The anodized titanium possess higher surface energy and wettability compared to as received titanium<sup>25</sup>. Furthermore, it has been suggested that titania with a 3-D nanoporous structure may enhance hydroxyapatite formation when compared to dense titania<sup>26</sup>. Osteoblast adhesion and activity is enhanced on rougher titanium surfaces than on the smoother surfaces. Rougher surfaces enhance osteoblast activity as there is an increased surface area available for cell (osteoblast) interaction. The studies in the past focused on modifying titanium surface at the microscale (10<sup>-6</sup> m) and nanoscale (10<sup>-9</sup> m) level. Therefore, fabrication of nanoscale structures (nanotubes) on the titanium substrates will provide a larger surface area than the microscale rough surface<sup>27</sup>.

The differential of our research was to evaluate the influence of anodization parameters such as voltage, time length and annealing temperature, on TiO<sub>2</sub> nanotubes formation on Ti-7.5Mo alloy surface. This alloy was chosen due to its excellent bulk properties in order to obtain a better surface.

## 2. Materials and Methods

The Ti-7.5Mo alloy was produced from sheets of commercially pure titanium (99.9%) and molybdenum (99.9%). Samples were melted in an arc furnace under an argon atmosphere. Ingots were homogenized under vacuum at 1100°C for 86.4 ks to eliminate chemical segregation. They were cold worked by swaging and bars with 13 mm of diameter were produced. Discs with 4 mm of thickness were cut and samples were divided into two groups according to the anodization potential, and each group into two subgroups according to the anodization time.

Sample were grinded with sandy papers (200 to 1200 mesh) and polished with a solution formed with colloidal silica (OPS – Sytuers) plus 5% oxalic acid. They were cleaned in the ultrasonic bath: 20 minutes in water, 20 minutes in alcohol and 20 minutes in acetone. The electrolyte used for anodization was glycerol containing 0.25% NH<sub>4</sub>F. The parameters used in the surface treatment are showed in Table 1. After the anodization, the samples were washed with deionized water, dried, and calcined for 1 hour at 450 °C or 600 °C at a heating rate of 5 °C per minute, and cooled in the oven.

Surfaces were evaluated by using a Field emission Gun - Scanning Electron microscope (SEM-FEG, XL 30 FEG, Philips) after anodization. The roughness of the TiO<sub>2</sub> nanotubes grow under different conditions were characterized using an atomic force microscope (AFM), VEECO Multimode V, operating in dynamic mode, with a 0.01–0.025-ohm.cm antimony-(n)-doped Si tip (model TESPW). The scanning area was 1 × 1 μm. The thickness of TiO<sub>2</sub> coating layers (nm) and average roughness (*Ra*) were determined using a surface area of 1 × 1 μm.

The structure of TiO<sub>2</sub> nanotubes was evaluated by X-ray diffraction (XRD), in a Siemens D5005 X-ray Diffractometer, using Cu-Kα radiation (λ=1.54056 Å) in the range of 2θ = 10°-90° at a scan rate of 1 deg/min.

Contact angle measurements were carried out to evaluate the wettability of the surfaces. The contact angle was obtained by using the sessile drop method on an advanced Rame-Hart goniometer, model n° 300-F1. The shape of the drop was recorded by a digital camera and the contact angles were measured from the images. The volume of each drop was 2 μl and the average value of at least 5 drops was calculated.

## 3. Results and Discussion

Anodizing conditions are important factors for the formation of aligned TiO<sub>2</sub> nanotubes. Among these conditions, the potential for anodizing applied plays an important role.

Figure 1 shows the image of the samples after anodization at 20V and 30V for 24 hours and 48 hours, annealed at 450 °C. A self-organized and homogeneous layer of the nanotubes was obtained in all evaluated conditions. For samples anodized at 20 V (Figure 1a and Figure 1c ) and 30 V (Figure 1b and Figure 1d), the average pore diameter was 80 nm and 100 nm, respectively. These results were similar to Lockman *et al.* (2010)<sup>28</sup> who concluded that the tube diameter is linearly dependent on the potential applied during the growth of nanotubes

According to Regonini *et al.* (2013)<sup>29</sup> for most electrolytes and with potencial ranging between 10 and 20V, TiO<sub>2</sub> nanotubes can be obtained with diameter between 50-100 nm. Out of these conditions, only irregular structures can be created. However, it has been reported that the pore diameter can be varied by altering the growth conditions such as the anodizing electrolyte and the potencial.

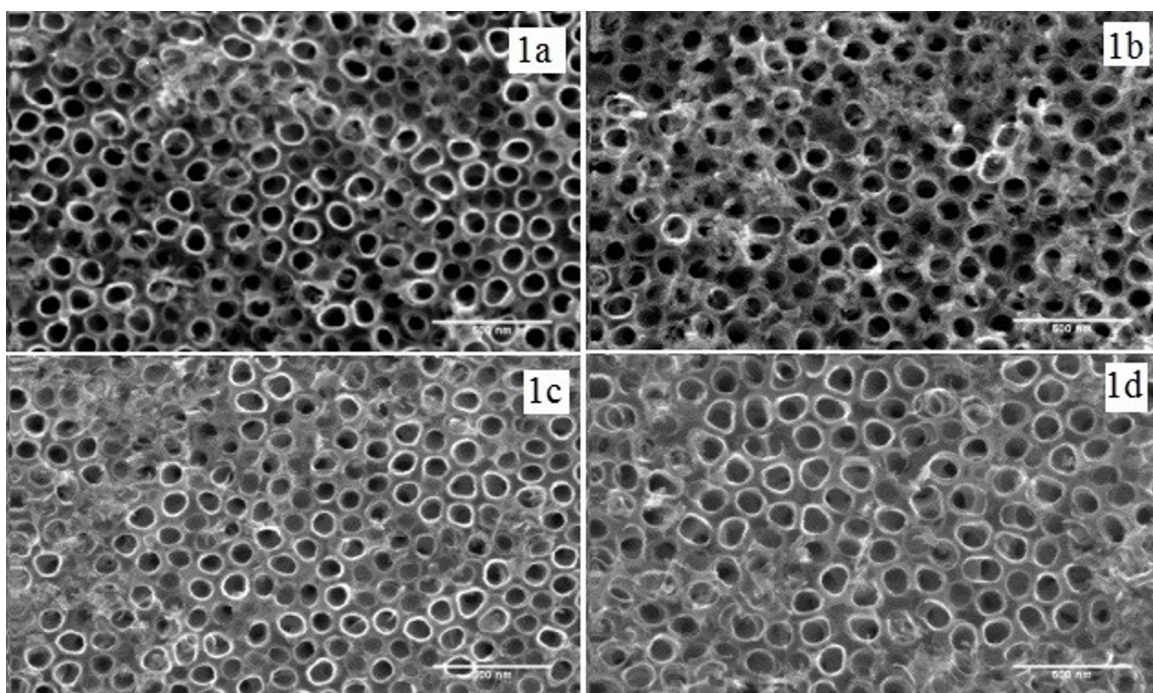
The increase of the potencial increases the diameter of the pores and is in accordance with other works carried out in pure Ti substrates<sup>30,31</sup>. Furthermore, in all such works on pure Ti foils, the arrangements of the individual TiO<sub>2</sub> nanotubes showed to be aligned and well separated. Moreover, Mohan *et al.* (2015)<sup>23</sup> verified that critical factors that affecting pore diameter depend on the alloy composition and the potencial anodizing.

The same parameters were evaluated for annealing at 600 °C for one hour. Figure 2 shows images of the samples anodized at 20V (Figure 2a and Figure 2c ) and 30V (Figure 1b and Figure 1d), for 24 hours and 48 hours, respectively. In this case, the use of this temperature influenced TiO<sub>2</sub> nanotube layers formation in only condition: 20 V for 24 hours (Figure 2a). This aspect of the surface was classified such as “protusions” by Varghese *et al.* (2003)<sup>21</sup>. In samples anodized at 20 V for 48 hours the nanotubes diameter was 60 nm.

The pore size of the 80 nm and 120 nm were obtained when 30 V was maintained for 24 hours (Figure 2b) and

**Table 1.** Surface properties of anodized Ti-7.5Mo

Anodization Conditions	Diameter and Thickness of TiO <sub>2</sub> coating layers (nm)	Median roughness (Ra) (nm)	Contact angle (degree)
20V - 24h - 450 °C	60 and 235	85 + 1.33	37.7
30V - 24h - 450 °C	100 and 277	53 + 1.30	30.2
20V - 48h - 450 °C	60 and 510	87 + 5.08	9.8
30V - 48h - 450 °C	100 and 639	57 + 1.28	15.3
20V - 24h - 600 °C	80 and 234	73 + 0.92	16.1
30V - 24h - 600 °C	120 and 239	41 + 1.57	14.4
20V - 48h - 600 °C	80 and 329	75 + 0.90	17.2
30V - 48h - 600 °C	120 and 564	44 + 1.52	12.2

**Figure 1.** SEM micrographs of the Ti-7.5Mo alloy after anodization at 20V and 30V for 24 hours and 48 hours, calcined at 450 °C: samples anodized at 20 V (1a and 1c) and 30 V (1b and 1d)

48 hours (Figure 2d), respectively. According Macak *et al.* (2008)<sup>32</sup>, the diameter changes linearly with the potential applied during the growth of nanotubes and it was observed in our results.

In order to evaluate the cristallinity of the tubes at different potencial, a series of experiments was performed. Figure 3 shows the X-ray diffraction patterns for the samples annealed calcined at 450 °C in which the presence of peaks of titanium substrate and the anatase phase can be observed. In the same way Chavez *et al.* (2016)<sup>33</sup>, the anatase phase formation was verified in all the samples under the same heat treatment, altering only the anodizing potential. Otherwise, in the samples annealed at 600 °C (Figure 4), there is the presence of peaks of titanium, anatase and rutile phases.

It is already well known that the arrangement of TiO<sub>2</sub> nanotubes formed is an amorphous structure, and with the heat treatment at high temperatures and with the presence of oxygen, the nanotubes become anatase phase, and the layer of metal under the nanotubes changes to rutile, and the perceived crystalline phases are polycrystalline<sup>34</sup>. However, there are divergences in which temperatures these different phases are formed.

In previous work<sup>35</sup>, done with pure titanium, TiO<sub>2</sub> nanotubes presented the anatase crystalline phase in samples treated at 280 °C. At 430 °C the anatase phase formed completely and a small rutile peak appeared, while at 620 °C only the rutile peak was present. In the other hand, the work of Mohan *et al.* (2015)<sup>23</sup> observed the presence of the anatase phase after

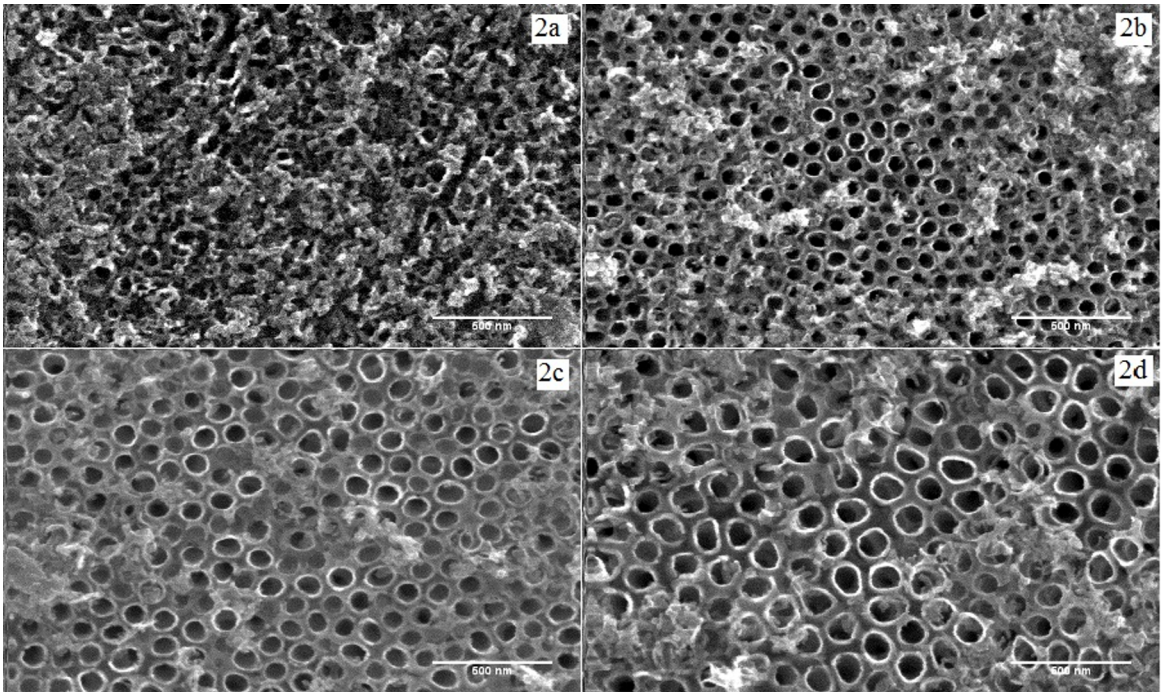
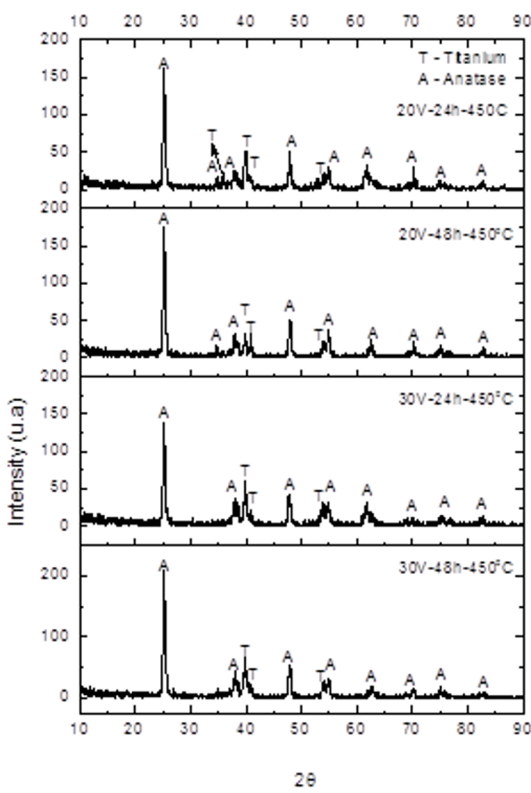
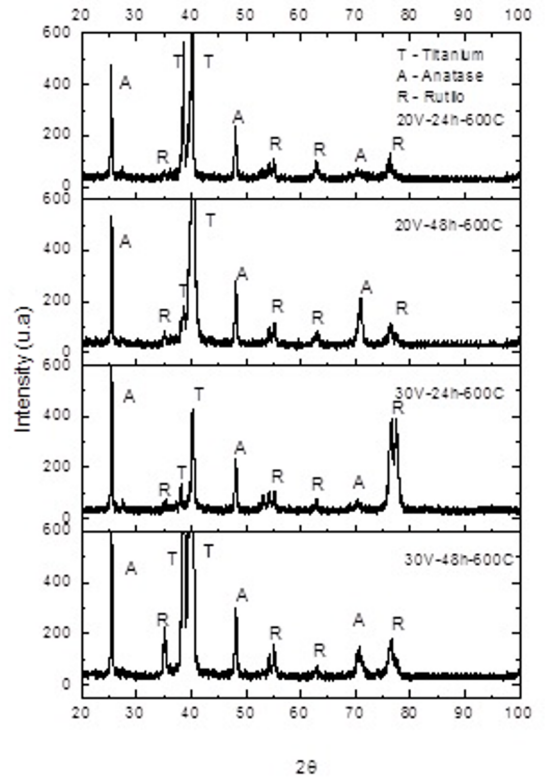


**Figure 2.** SEM micrographs of the Ti-7.5Mo alloy after anodization at 20V and 30V for 24 hours and 48 hours, calcined at 600 °C: samples anodized at 20 V (2a and 2c) and 30 V (2b and 2d)



**Figures 3.** The X-ray diffraction patterns for the samples calcined at 450 °C.



**Figures 4.** The X-ray diffraction patterns for the samples calcined at 600 °C

heat treatment between 450 and 600 °C. In samples treated at 700 °C, part of the anatase turned into a rutile phase, and only at 850 °C the dominant phase was rutile.

AFM images revealed distinct topography for all samples. Figure 5 shows the images of the samples anodized at 20V and 30V, for 24 and 48 hours and annealed at 450 °C for 1 hour. Figures 5 (a) and 5 (c) are related to samples anodized for 24 hours, and figures 5 (b) and 5 (d) the samples anodized for 48 hours. Figure 6 shows the images of the samples anodized at 20V and 30V, and annealed at 600 °C for 1 hour. Figures 6 (a) and 6 (c) are related to samples anodized for 24 hours, and Figures 6 (b) and 6 (d) the samples anodized for 48 hours.

With the AFM analysis, it was possible to obtain the average roughness (Ra) and the thickness of the titania layer formed on the surface as shown in Table 1. When comparing the thickness of the titania layer obtained, it is observed that the highest thickness was obtained in samples anodized for 48 hours, while the samples anodized for 24 hours exhibited smallest thickness. These results are in accordance with Narayanan et al., (2009)<sup>36</sup>, where they were concluded that the anodization time affected the nanotube length, thereby, the thickness of the layer TiO<sub>2</sub> formed. Our study showed the surface roughness decreases with increasing nanotubes diameter and differs from the study of Yu et al., (2010)<sup>37</sup>.

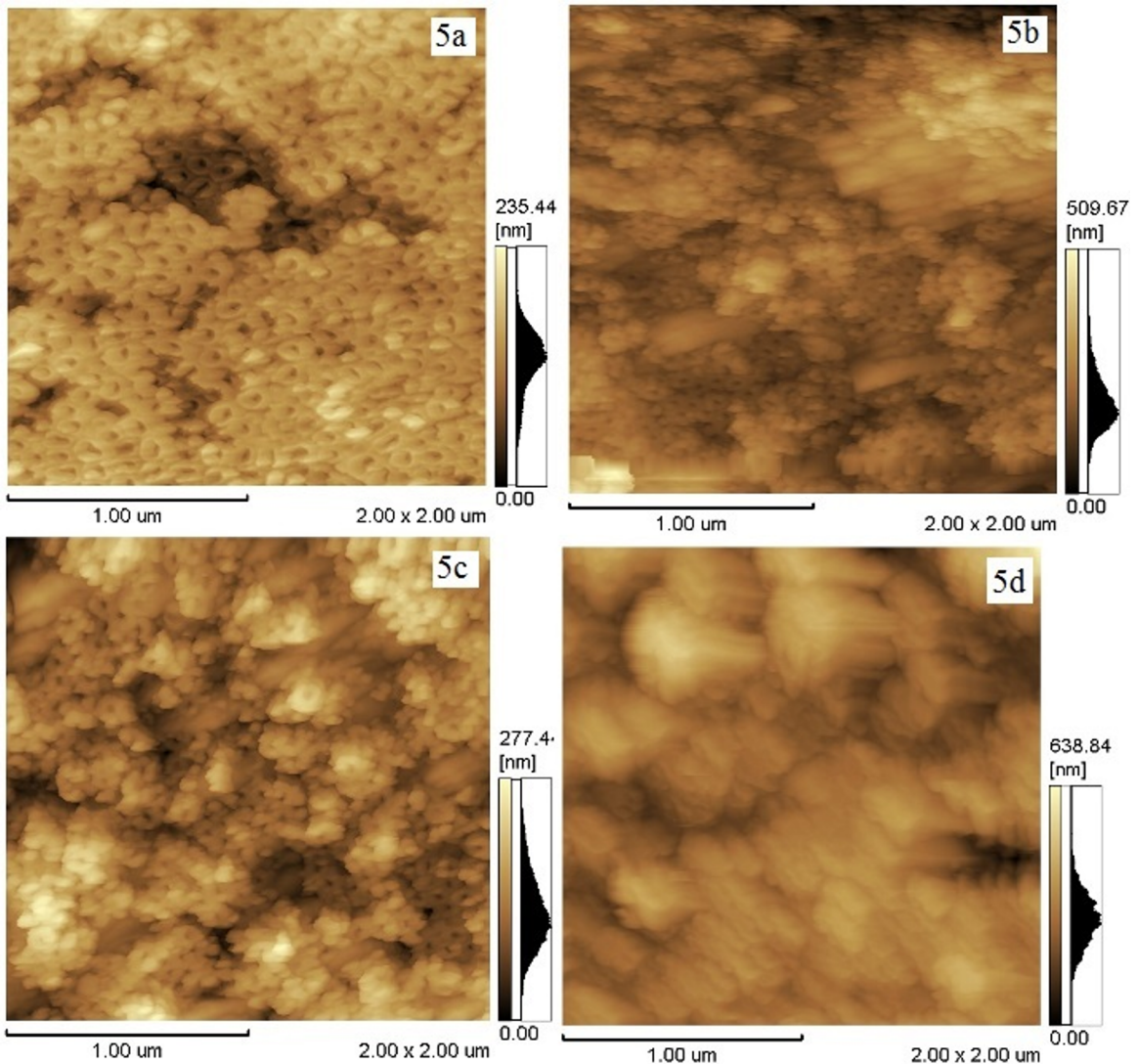


**Figure 5.** AFM images of the Ti-7.5Mo alloy after anodization at 20V and 30V and calcined at 450 °C: for 24 hours (5a and 5c) and for 48 hours (5b and 5d)

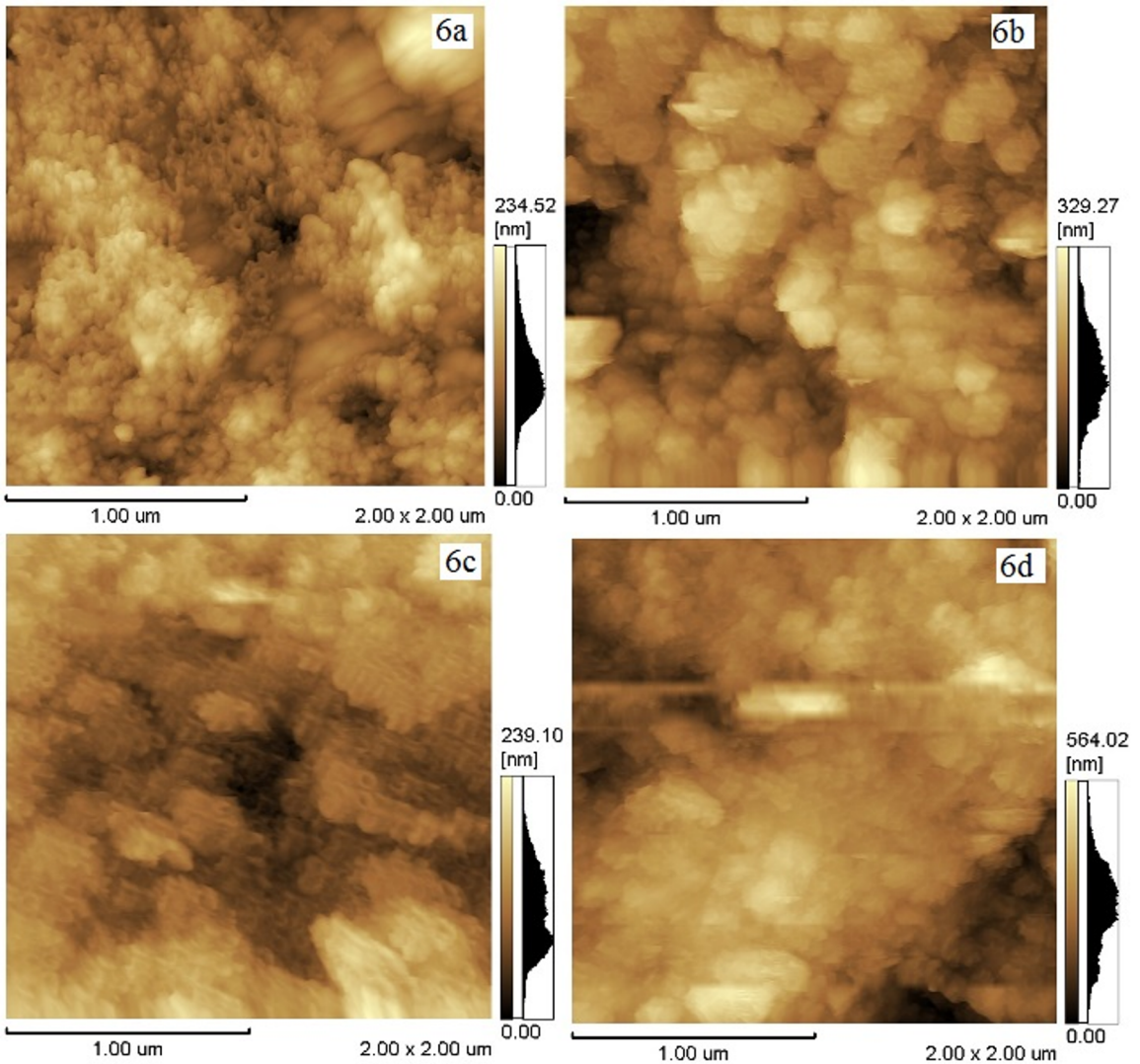


**Figure 6.** AFM images of the Ti-7.5Mo alloy after anodization at 20V and 30V and calcined at 600 °C: for 24 hours (5a and 5c) and for 48 hours (5b and 5d)

The ANOVA results complemented by Tukey's test indicated that the highest values were observed in the surface anodized at 20V (Table 2). The ANOVA results (three-way) indicated significant differences in the treatment ( $p < 0.001$ ) with higher values of surface roughness in the samples anodized at 20 V when compared to 30V. Also, there were significant differences in the temperature factor ( $p = 0.001$ ), with higher values of roughness in samples annealed at 450 °C. The different processes showed that neither time ( $p = 0.123$ ) nor temperature ( $p = 0.420$ ) (Table 3) influenced the results.

The water contact angles were used to investigate the wettability of TiO<sub>2</sub> nanotubes.

A variation in the contact angle between 37.7° and 9.8° was observed; however, the highest values are present in the samples annealed at 450 °C (Figure 7), while the lowest values are present in the samples annealed at 600 °C. That

probably happened because of the crystalline structure present in the anatase and rutile phases (samples annealed at 600°C), which made the film more hydrophilic than only the anatase phase than when only the anatase phase is present (samples annealed at 450 °C). This result is in line with the previous studies<sup>38</sup>.

Surface wettability (hydrophobicity/hydrophilicity) is one of the most important parameters affecting the biological response to an implanted biomaterial and has a profound influence on the cells behavior during the process of osseointegration, which begins when the implant is in contact with the blood.

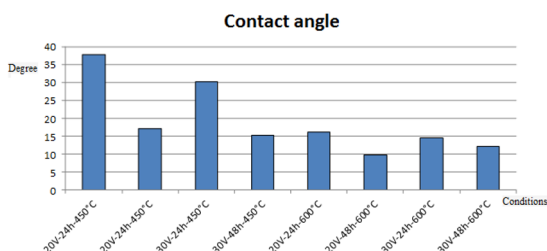
Wettability affects protein adsorption, platelet adhesion/activation, blood coagulation and cell and bacterial adhesion<sup>39</sup>. Highly hydrophilic surfaces seem more desirable than hydrophobic ones in view of their interactions with biological

**Table 2.** ANOVA results complemented with Tukey. Comparison between the roughness values in the different groups

Roughness Groups tested Average (DP)								ANOVA	
20v	20v	20v	20v	30v	30v	30v	30v	F	P
24h	48h	24h	48h	24h	48h	24h	48h		
450°C	450°C	600°C	600°C	450°C	450°C	600°C	600°C		
76.288	90.421	61.552	70.703	48.370	42.978	32.836	36.779	14.098	<0.001
(7.618)	(2.602)	(13.472)	(7.906)	(13.170)	(19.017)	(8.930)	(6.003)		

**Table 3.** ANOVA results (three-way)

Variation source	DF	SS	MS	F	P
treatment	1	9522.276	9522.276	79.381	<0.001
time	1	238.384	238.384	1.987	0.171
temperature	1	1578.518	1578.518	13.159	0.001
treatment x time	1	305.885	305.885	2.550	0.123
treatment x temperature	1	80.918	80.918	0.675	0.420
time x temperature	1	9.476	9.476	0.0790	0.781
treatment x tempo x temperature	1	102.481	102.481	0.854	0.365
Residual	24	2878.973	119.957		
Total	31	14716.911	474.739		

**Figure 7.** Contact angle measurements for all conditions studied

fluids, cells and tissues<sup>40</sup>. According to Elias *et al.*<sup>41</sup>, the adsorption behavior and protein adhesion on the implant surface depends on the surface properties. On hydrophobic surfaces, traces of antibodies reduce cell adsorption. On hydrophilic surfaces, traces of thrombin and prothrombin predominate and increase the cellular adsorption. Therefore, in order to promote the proliferation of human osteoblasts, it is necessary to increase the surface area of the implant, which consequently increases the wettability of the surface. This increased wettability results in increased cell proliferation, indicating the importance of hydrophilicity for applications such as dental implants. Furthermore, according to Lim and Donahue<sup>42</sup>, the relationship between the contact angle and wettability are inversely related on the same surface. Therefore, a decrease of this angle increases the capacity for surface wettability. With the contact angle ranging

from 37.7 ° to 9.8 °, it's possible to conclude that, the best condition for wettability was obtained in samples anodized at 20V-48h-450 °C.

## 4. Conclusions

In this paper, the effects of anodizing potential and time, and annealing temperature of the growth of TiO<sub>2</sub> nanotubes were investigated. It was found that anodizing time was the critical parameter for controlling the growth of nanotube and the anodizing potential contributed to change diameter of the nanotubes. Self-organized nano-tubular TiO<sub>2</sub> layer was formed on Ti-7.5Mo alloy from electrolyte containing glycerol and 0.25 % NH<sub>4</sub>F. In the samples anodized at 20 V the average pore diameter was 80 nm, while for samples anodized at 30 V average pore diameter was 110 nm. In all groups annealed at 450 °C there was only anatase phase and for the samples annealed at 600 °C, there is the presence of peaks of titanium, anatase and rutile phases. The AFM and contact angle measurements showed that the samples anodized at 20 V presented the highest surface roughness (~87 nm) and best hydrophilicity (~9.8°). From those results, it is possible to conclude that the best condition to use as biomaterial was 20V, 48h and 450 °C due to the presence of the anatase phase, the highest surface roughness and best hydrophilicity.

## 5. Acknowledgments

The authors acknowledge financial support received from FAPESP (Project 2013 / 08200 – 9).

## 6. References

- Black J, Hasting G. *Handbook of Biomaterial Properties*. London: Chapman & Hall; 1998. p. 179-200.
- Ratner BD, Hoffman AS, Schoen FJ, Lemons JE. *Biomaterials Science. An Introduction to Materials in Medicine*. San Diego: Academic Press; 1997.
- Escada ALA, Machado JPB, Schneider SG, Rezende MCRA, Claro APRA. Biomimetic calcium phosphate coating on Ti-7.5Mo alloy for dental application. *Journal of Materials Science: Materials in Medicine*. 2011;22(11):2457-2465.
- Escada ALA, Rodrigues Jr. D, Claro APRA. Surface characterization of Ti 7.5Mo alloy modified by biomimetic method. *Surface & Coatings Technology*. 2010;205(2):383-387.
- Alves APR, Santana FA, Rosa LAA, Cursino SA, Codaro EN. A study on corrosion resistance of the Ti-10Mo experimental alloy after different processing methods. *Materials Science and Engineering: C*. 2004;24(5):693-696.
- Rezende MCRA, Alves APR, Codaro EN, Dutra CAM. Effect of commercial mouthwashes on the corrosion resistance of Ti-10Mo experimental alloy. *Journal of Materials Science: Materials in Medicine*. 2007;18(1):149-154.
- Lin DJ, Chuang CC, Chern Lin JH, Lee JW, Ju CP, Yin HS. Bone formation at the surface of low modulus Ti-7.5Mo implants in rabbit femur. *Biomaterials*. 2007;28(16):2582-2589.
- Lin CW, Ju CP, Chern Lin JH. A comparison of the fatigue behavior of cast Ti-7.5Mo with c.p. titanium, Ti-6Al-4V and Ti-13Nb-13Zr alloys. *Biomaterials*. 2005;26(16):2899-2907.
- Niemeyer TG, Grandini CR, Pinto LMC, Angelo ACD, Schneider SG. Corrosion behavior of Ti-13Nb-13Zr alloy used as a biomaterial. *Journal of Alloys and Compounds*. 2009;476(1-2):172-175.
- Sumner DR, Turner TM, Igloria R, Urban RM, Galante JO. Functional adaptation and ingrowth of bone vary as a function of hip implant stiffness. *Journal of Biomechanics*. 1998;31(10):909-917.
- Pang YL, Abdullah AZ. Effect of low Fe<sup>3+</sup> doping on characteristics, sonocatalytic activity and reusability of TiO<sub>2</sub> nanotubes catalysts for removal of Rhodamine B from water. *Journal of Hazardous Materials*. 2012;235-236:326-335.
- El Saeed AM, El-Fattah MA, Dardir MM. Synthesis and characterization of titanium oxide nanotubes and its performance in epoxy nanocomposite coating. *Progress in Organic Coatings*. 2015;78:83-89.
- Erjavec B, Kaplan R, Pintar A. Effects of heat and peroxide treatment of photocatalytic activity of titanate nanotubes. *Catalysis Today*. 2015;241(Pt A):15-24.
- Wang T, Wei J, Shi H, Zhou M, Zhang Y, Chen Q, et al. Preparation of electrospun Ag/TiO<sub>2</sub> nanotubes with enhanced photocatalytic activity based on water/oil phase separation. *Physica E: Low-dimensional Systems and Nanostructures*. 2017;86:103-110.
- Hosseini MG, Momeni MM. UV-cleaning properties of Pt nanoparticle-decorated titania nanotubes in the electro-oxidation of methanol: An anti-poisoning and refreshable electrode. *Electrochimica Acta*. 2012;70:1-9.
- Chen K, Feng X, Hu R, Li Y, Xie K, Li Y, et al. Effect of Ag nanoparticle size on the photoelectrochemical properties of Ag decorated TiO<sub>2</sub> nanotube arrays. *Journal of Alloys and Compounds*. 2013;554:72-79.
- Textor M, Sittig C, Frauchiger V, Tosatti S, Brunnete DM. Properties and Biological Significance of Natural Oxide Films on Titanium and its Alloys In: Brunnete DM, Tengvall P, Textor M, Thomsen P, eds. *Titanium in Medicine*. New York: Springer; 2001. p. 171-230.
- He H, Xiao P, Zhou M, Liu F, Yu S, Qiao L, et al. PtNi alloy nanoparticles supported on carbon-doped TiO<sub>2</sub> nanotube arrays for photo-assisted methanol oxidation. *Electrochimica Acta*. 2013;88:782-789.
- Lai CW, Sreekantan S. Incorporation of WO<sub>3</sub> species into TiO<sub>2</sub> nanotubes via wet impregnation and their water-splitting performance. *Electrochimica Acta*. 2013;87:294-302.
- Macak JM, Tsuchiya H, Ghicov A, Yasuda K, Hahn R, Bauer S, et al. TiO<sub>2</sub> nanotubes: Self-organized electrochemical formation, properties and applications. *Current Opinion in Solid State and Materials Science*. 2007;11(1-2):3-18.
- Varghese OK, Gong D, Paulose M, Grimes CA, Dickey EC. Crystallization and high-temperature structural stability of titanium oxide nanotube arrays. *Journal of Materials Research*. 2003;18(1):156-165.
- Bauer S, Pittrof A, Tsuchiya H, Schmuki P. Size-effects in TiO<sub>2</sub> nanotubes: Diameter dependent anatase/rutile stabilization. *Electrochemistry Communications*. 2011;13(6):538-541.
- Mohan L, Anandan C, Rajendran N. Electrochemical behavior and effect of heat treatment on morphology, crystalline structure of self-organized TiO<sub>2</sub> nanotube arrays on Ti-6Al-7Nb for biomedical applications. *Materials Science and Engineering: C*. 2015;50:394-401.
- Yao C, Perla V, McKenzie JL, Slamovich EB, Webster TJ. Anodized Ti and Ti<sub>6</sub>Al<sub>4</sub>V Possessing Nanometer Surface Features Enhances Osteoblast Adhesion. *Journal of Biomedical Nanotechnology*. 2005;1(1):68-73.
- Zhu X, Chen J, Scheideler L, Reichl R, Geis-Gerstorfer J. Effects of topography and composition of titanium surface oxides on osteoblast responses. *Biomaterials*. 2004;25(18):4087-4103.
- Yang B, Uchida M, Kim HM, Zhang X, Kokubo T. Preparation of bioactive titanium metal via anodic oxidation treatment. *Biomaterials*. 2004;25(6):1003-1010.
- Zwilling V, Aucouturier M, Darque-Ceretti E. Anodic oxidation of titanium and TA6V alloy in chromic media. An electrochemical approach. *Electrochimica Acta*. 1999;45(6):921-929.



28. Lockman Z, Sreekantan S, Ismail S, Schmidt-Mende L, MacManus-Driscoll JL. Influence of anodisation voltage on the dimension of titania nanotubes. *Journal of Alloys and Compounds*. 2010;503(2):359-364.
29. Regonini D, Bowen CR, Jaroenworarluck A, Stevens R. A review of growth mechanism, structure and crystallinity of anodized TiO<sub>2</sub> nanotubes. *Materials Science and Engineering: R: Reports*. 2013;74(12):377-406.
30. Crawford GA, Chawla N. Tailoring TiO<sub>2</sub> nanotube growth during anodic oxidation by crystallographic orientation of Ti. *Scripta Materialia*. 2009;60(10):874-877.
31. Cai Q, Yanga L, Yu Y. Investigations on the self-organized growth of TiO<sub>2</sub> nanotube arrays by anodic oxidation. *Thin Solid Films*. 2006;515(4):1802-1806.
32. Macak JM, Hildebrand H, Marten-Jahns U, Schmuki P. Mechanistic aspects and growth of large diameter self-organized TiO<sub>2</sub> nanotubes. *Journal of Electroanalytical Chemistry*. 2008;621(2):254-266.
33. Chaves JM, Escada ALA, Alves Claro APR. Characterization of the structure, thermal stability and wettability of the TiO<sub>2</sub> nanotubes growth on the Ti-7.5Mo alloy surface. *Applied Surface Science*. 2016;370:76-82.
34. Zhao J, Wang X, Sun T, Li L. In situ templated synthesis of anatase single-crystal nanotube arrays. *Nanotechnology*. 2005;16(10):2450-2454.
35. Zalnezhad E, Hamouda AMS, Farajc G, Shamshirband S. TiO<sub>2</sub> nanotube coating on stainless steel 304 for biomedical applications. *Ceramics International*. 2015;41(2 Pt B):2785-2793.
36. Narayan R, Kwon TB, Kim KH. TiO<sub>2</sub> nanotubes from stirred glycerol/NH<sub>4</sub>F electrolyte: Roughness, wetting behavior and adhesion for implant applications. *Materials Chemistry and Physics*. 2009;117(2-3):460-464.
37. Yu W, Jiang X, Zhang F, Xu L. The effect of anatase TiO<sub>2</sub> nanotube layers on MC3T3-E1 preosteoblast adhesion, proliferation, and differentiation. *Journal of Biomedical Materials Research Part A*. 2010;94A(4):1012-1022.
38. Anitha VC, Lee JH, Lee J, Banerjee AN, Joo SW, Min BK. Biofilm formation on a TiO<sub>2</sub> nanotube with controlled pore diameter and surface wettability. *Nanotechnology*. 2015;26(6):065102.
39. Choe JH, Lee SJ, Lee YM, Rhee JM, Lee HB, Khang G. Proliferation Rate of Fibroblast Cells on Polyethylene Surfaces with Wettability Gradient. *Journal of Applied Polymer Science*. 2004;92(1):599-606.
40. Bohner M, Gasser B, Baroud G, Heini P. Theoretical and experimental model to describe the injection of a polymethylmethacrylate cement into a porous structure. *Biomaterials*. 2004;24(16):2721-2730.
41. Elias CN, Lima JHC, Valiev R, Meyers MA. Biomedical applications of titanium and its alloys. *JOM*. 2008;60(3):46-49.
42. Lim JY, Donahue HJ. Biomaterial characteristics important to skeletal tissue engineering. *Journal of Musculoskeletal & Neuronal Interactions*. 2004;4(4):396-398.